Research Article

Vol. 26, No. 9 | 30 Apr 2018 | OPTICS EXPRESS 11171

Optics EXPRESS

# Transverse modal control of wide-stripe high power semiconductor lasers using sampled grating

LIANYAN LI,[1,2] YUECHUN SHI,[2,*] YONG ZHAO,[2] YUNSHAN ZHANG,[1,2] WENXUAN WANG,[2] YITAO WU,[2] YINLI ZHOU,[3] XING ZHANG,[3] AND XIANGFEI CHEN[2]

[1]*College of Electronic and Optical Engineering & College of Microelectronics, Nanjing University of Posts and Telecommunications, Nanjing 210023, China*
[2]*College of Engineering and Applied Sciences, Nanjing University, Nanjing 210009, China*
[3]*State Key Laboratory of Luminescence and Application, Changchun Institute of Optics, Fine Mechanics and Physics, Chinese Academy of Sciences, Changchun 130033, China*
**shiyc@nju.edu.cn*

**Abstract:** A transverse Bragg resonance (TBR) waveguide semiconductor laser with sampled grating is proposed and analyzed. The transverse phase shift in the middle of the grating is realized by shifting half of the sampling period, resulting in a good single transverse mode resonance. The characteristics such as the modal gain, the electric field distribution, the near and far field beam patterns are theoretically studied. Since the sampled grating is designed by combining a uniform basic grating with a micrometer scale sampling pattern, it can be easily fabricated by holographic exposure and conventional photolithography with low cost. Therefore, the proposed method would be beneficial to volume fabrication of wide-stripe high power semiconductor lasers.



**OCIS codes:** (140.0140) Lasers and laser optics; (050.2770) Gratings.

## References and links

1. L. Zhu, A. Scherer, and A. Yariv, "Modal gain analysis of transverse Bragg resonance waveguide lasers with and without transverse defects," IEEE J. Quantum Electron. **43**(10), 934–940 (2007).
2. R. J. Lang, D. Mehuys, D. F. Welch, and L. Goldberg, "Spontaneous filament formation in broad area diode laser amplifiers," IEEE J. Quantum Electron. **30**(3), 685–694 (1994).
3. R. J. Lang, K. Dzurko, A. Hardy, S. Demars, A. Schoenfelder, and D. F. Welch, "Theory of Grating-Confined Broad-Area Lasers," IEEE J. Quantum Electron. **34**(11), 2196–2210 (1998).
4. Y. Zhu, Y. Zhao, and L. Zhu, "Two-dimensional photonic crystal Bragg lasers with triangular lattice for monolithic coherent beam combining," Sci. Rep. **7**(1), 10610 (2017).
5. A. M. Sarangan, M. W. Wright, J. R. Marciante, and D. J. Bossert, "Spectral Properties of Angled-Grating High-Power Semiconductor Lasers," IEEE J. Quantum Electron. **35**(8), 1220–1230 (1999).
6. L. Zhu, G. A. Derose, A. Scherer, and A. Yariv, "Electrically pumped edge-emitting photonic crystal lasers with angled facets," Opt. Lett. **32**(10), 1256–1258 (2007).
7. P. Yeh and A. Yariv, "Bragg reflection waveguides," Opt. Commun. **19**(3), 427–430 (1976).
8. J.-S. Lee and S.-Y. Shin, "Strong discrimination of transverse modes in high-power laser diodes using Bragg channel waveguiding," Opt. Lett. **14**(2), 143–145 (1989).
9. A. Yariv, Y. Xu, and S. Mookherjea, "Transverse Bragg resonance laser amplifier," Opt. Lett. **28**(3), 176–178 (2003).
10. W. Liang, Y. Xu, J. M. Choi, and A. Yariv, "Engineering transverse Bragg resonance waveguides for large modal volume lasers," Opt. Lett. **28**(21), 2079–2081 (2003).
11. A. Yariv, "Coupled-wave formalism for optical waveguiding by transverse Bragg reflection," Opt. Lett. **27**(11), 936–938 (2002).
12. L. Zhu, J. M. Choi, G. A. DeRose, A. Yariv, and A. Scherer, "Electrically pumped two-dimensional Bragg grating lasers," Opt. Lett. **31**(12), 1863–1865 (2006).
13. Y. Dai and X. Chen, "DFB semiconductor lasers based on reconstruction-equivalent-chirp technology," Opt. Express **15**(5), 2348–2353 (2007).
14. Y. Shi, S. Li, X. Chen, L. Li, J. Li, T. Zhang, J. Zheng, Y. Zhang, S. Tang, L. Hou, J. H. Marsh, and B. Qiu, "High channel count and high precision channel spacing multi-wavelength laser array for future PICs," Sci. Rep. **4**(1), 7377 (2015).

#322861 https://doi.org/10.1364/OE.26.011171
Journal © 2018 Received 9 Feb 2018; revised 11 Apr 2018; accepted 11 Apr 2018; published 16 Apr 2018

15. Y. Shi, S. Li, J. Li, L. Jia, S. Liu, and X. Chen, "An apodized DFB semiconductor laser realized by varying duty cycle of sampling Bragg grating and reconstruction-equivalent-chirp technology," Opt. Commun. **283**(9), 1840–1844 (2010).
16. H. Ghafouri-Shiraz, *Distributed feedback laser diodes and optical tunable filters* (Wiley, 2003).
17. D. Marcuse, "Reflection loss of laser mode from tilted end mirror," J. Lightwave Technol. **7**(2), 336–339 (1989).
18. J. M. Choi, *Design, fabrication, and characterization of semiconductor transverse Bragg resonance lasers*, (Ph.D. dissertation, California Institute of Technology, 2007).
19. Y. Shi, X. Tu, S. Li, Y. Zhou, L. Jia, and X. Chen, "Numerical study of three phase shifts and dual corrugation pitch modulated (CPM) DFB semiconductor lasers based on reconstruction equivalent chirp technology," Chin. Sci. Bull. **55**(35), 4083–4088 (2010).

## 1. Introduction

Total internal reflection (TIR) is the most commonly used waveguiding mechanism for wide-stripe high power semiconductor lasers. However, it requires a very small refractive index contrast for single mode operation and suffers from self-focusing nonlinearity, leading to the formation of localized hot spots or filaments [1–3]. Therefore, continuous-wave diffraction-limited high power semiconductor lasers are usually elusive and have attracted much attention [4–6]. In order to control the transverse mode and mitigate the filamentation effects of wide-stripe high power semiconductor lasers, an optical waveguiding mechanism based on Bragg reflection rather than TIR has been proposed, which is called a transverse Bragg resonance (TBR) waveguide [7–10].

Two kinds of TBR waveguides have been studied up to now. One is the angled-grating distributed feedback laser (α-laser) proposed by Lang, et al [3]. It uses angled uniform grating as a continuous spatial filter to realize transverse resonance. Due to the wide grating width in the transverse direction, this kind of laser can achieve diffraction-limited high output power. However, the α-laser has two degenerated modes, which can beat along the cavity to form a snaking mode pattern. Therefore, the laser cavity length must be carefully controlled to be multiple times of the beat length in order to achieve a strong facet feedback. The other type of TBR waveguide was proposed by Yariv [11], in which a line defect (grating phase shift) is inserted in the middle of the grating. As a result, a strong resonance with reduced radiation loss along the transverse direction can be realized. An electrically pumped TBR laser with single mode has been experimentally reported [12]. However, because of the small size of the line defect, the fabrication is usually realized by E-beam lithography (EBL) with high cost.

In this study, we propose a TBR waveguide with sampling structure and uniform basic grating to relax the fabrication precision requirement. The effect of the phase shift is equivalently realized by shifting half of the sampling period, which can be designed in micrometer scale [13,14]. The proposed sampled grating can be fabricated by holographic exposure combining with conventional photolithography. Thus, the cost of such kind of high power semiconductor lasers can be considerably reduced.

## 2. Principle

The schematic of the proposed laser is shown in Fig. 1(a). The material stack is similar to the common distributed feedback (DFB) semiconductor lasers. It mainly consists of an n-InP substrate, a low separate confinement heterostructure (SCH) layer, a multiple quantum well (MQW) layer, an upper SCH layer and a p-InP layer. The sampled grating is patterned in the p-InP layer with the trenches filled with benzocyclobutene (BCB). The top view of the grating is shown in Fig. 1(b). Since the grating exits in only half period of the sampled grating in the p type InP layer, the contact resistance of the proposed device decreases comparing with the uniform grating if they have the same cavity width.

Optics EXPRESS

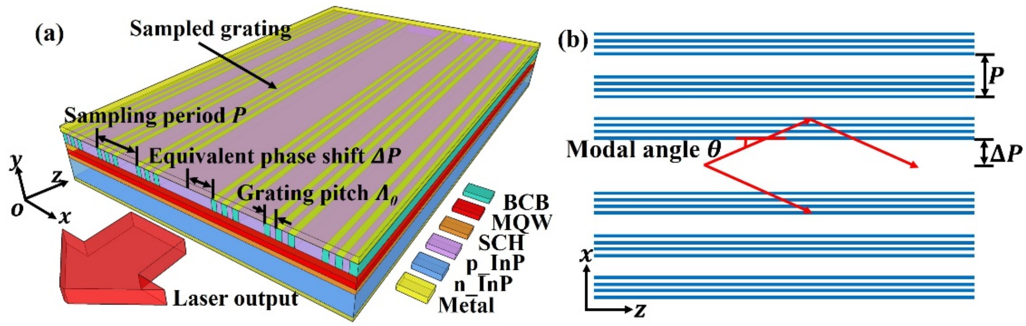


Fig. 1. (a) Schematic of the proposed TBR waveguide laser; (b) the top view of the sampled grating.

In the proposed structure, the grating is used to confine light in the transverse direction as a waveguide. The dielectric constant along the transverse direction can be expressed as,

$$\varepsilon(x) = \varepsilon_{r0} + \Delta\varepsilon(x) + i\varepsilon_i(x) \tag{1}$$

where $\varepsilon_{r0}$ is the average dielectric constant, $\Delta\varepsilon(x)$ is the dielectric constant modulation and $\varepsilon_i(x)$ indicates the material gain or loss.

Regarding the sampled grating shown in Fig. 1(b), the dielectric constant modulation can be expressed as,

$$\Delta\varepsilon(x) = \frac{1}{2}S(x)\left[\Delta\varepsilon_0 \exp\left(i\frac{2\pi}{\Lambda_0}x\right) + c.c\right] \tag{2}$$

where $\Delta\varepsilon_0$ is the amplitude of dielectric constant modulation, $\Lambda_0$ is the pitch of the basic grating, and $S(x)$ is the sampling function which can be Fourier expanded as,

$$S(x) = \sum s_m \exp\left(i\frac{2\pi m}{P}x\right) \tag{3}$$

where $s_m$ is Fourier coefficient and $P$ is the sampling period. Then the dielectric constant modulation can be modified as,

$$\Delta\varepsilon(x) = \frac{1}{2}\sum s_m\left[\Delta\varepsilon_0 \exp\left(i\frac{2\pi}{\Lambda_0}x + i\frac{2\pi m}{P}x\right) + c.c\right] \tag{4}$$

The sampled grating can be considered as a superposition of many subgratings with different grating period $\Lambda_m$ which satisfies,

$$\frac{1}{\Lambda_m} = \frac{1}{\Lambda_0} + \frac{m}{P} \tag{5}$$

If we consider the + 1st order subgrating, the dielectric constant modulation can be written as,

$$\Delta\varepsilon_{+1}(x) = \frac{1}{2}\Delta\varepsilon_0 s_{+1} \exp\left[i2\pi\left(\frac{1}{\Lambda_0} + \frac{1}{P}\right)x\right] + c.c \tag{6}$$

where $s_{+1}$ is the Fourier coefficient of the + 1st order subgrating, which is related to the duty cycle of the sampling structure [15].

If half of the sampling period $\Delta P = P/2$ is shifted in the sampling structure, the dielectric constant modulation can be modified as,

$$\Delta\varepsilon_{+1}(x)=\begin{cases}\frac{1}{2}\Delta\varepsilon_0 s_{+1}\exp\left[i2\pi\left(\frac{1}{\Lambda_0}+\frac{1}{P}\right)x\right]+c.c, x<x_0\\ \frac{1}{2}\Delta\varepsilon_0 s_{+1}\exp\left[i2\pi\left(\frac{1}{\Lambda_0}+\frac{1}{P}\right)x\right]\exp\left(i2\pi\frac{\Delta P}{P}x\right)+c.c, x\geq x_0\end{cases}\tag{7}$$

where $x_0$ is the position of the shift. Then an equivalent π phase shift can be obtained.

According to the coupled mode theory, there is a dominant TBR mode induced by the equivalent π phase shift [1]. It can propagate along the longitudinal direction with a specific complex propagation constant $\beta=\beta_r+i\beta_i$. The real part of the propagation constant $\beta_r$ can be expressed as,

$$\beta_{r(+1)}=k_0 n\sqrt{1-\left[\frac{\lambda}{2n}\left(\frac{1}{\Lambda_0}+\frac{1}{P}\right)\right]^2}\tag{8}$$

where $k_0$ is the grating vector in vacuum and $n$ is the effective index of the waveguide. The imaginary part of the propagation constant $\beta_i$ is defined as the modal gain, which means the modal gain or loss in the longitudinal direction.

It should be noted that the TBR waveguide with equivalent π phase shift is different from the common π phase-shifted TBR waveguide with only one dominant transverse mode. The proposed structure can be regarded as a four-mode waveguide, which can support the −1st and 0th order resonances except for the + 1st order resonance.

The dielectric constant modulation of the −1st order subgrating can be expressed as,

$$\Delta\varepsilon_{-1}(x)=\begin{cases}\frac{1}{2}\Delta\varepsilon_0 s_{-1}\exp\left[i2\pi\left(\frac{1}{\Lambda_0}-\frac{1}{P}\right)x\right]+c.c, x<x_0\\ \frac{1}{2}\Delta\varepsilon_0 s_{-1}\exp\left[i2\pi\left(\frac{1}{\Lambda_0}-\frac{1}{P}\right)x\right]\exp\left(-i2\pi\frac{\Delta P}{P}x\right)+c.c, x\geq x_0\end{cases}\tag{9}$$

Similar as the + 1$^{st}$ order subgrating, an equivalent π phase shift is also introduced at the position of $x_0$ as well as the corresponding transverse resonance mode. As a result, a TBR guided mode can also be set up in the proposed waveguide. Comparing with the + 1$^{st}$ order subgrating, its propagation constant $\beta_r$ can be expressed as,

$$\beta_{r(-1)}=k_0 n\sqrt{1-\left[\frac{\lambda}{2n}\left(\frac{1}{\Lambda_0}-\frac{1}{P}\right)\right]^2}\tag{10}$$

In addition, the dielectric constant modulation of the 0$^{th}$ order subgrating can be written as,

$$\Delta\varepsilon_0(x)=\frac{1}{2}\Delta\varepsilon_0 s_0\exp\left(i2\pi\frac{1}{\Lambda_0}x\right)+c.c\tag{11}$$

There are two degenerated modes at the two edges of the stopband of the 0$^{th}$ order subgrating, which is a uniform grating according to Eq. (11). The propagation constants $\beta_r$ of the two modes can be expressed as,

$$\beta_{r(0)}=k_0 n\left[\sqrt{1-\left(\frac{\lambda}{2n\Lambda_0}\right)^2}\pm\frac{2\Delta n\Lambda_0}{\pi\lambda}\right]\tag{12}$$

Therefore, the proposed TBR waveguide can be considered as a four-mode waveguide. When it is applied in the semiconductor laser, a spatial filter should be used to select one mode if single mode resonance is required. In this paper, an angled facet is preferred and analyzed for single mode light resonance, which will be discussed in the following.

## 3. Design and simulation results

The schematic of the TBR laser based on sampled grating is shown in Fig. 1. The parameters used in the design are listed in Table 1. The $0^{th}$ order wavelength or the $\pm$ $1^{st}$ order wavelength $\lambda_{0,\pm1}$ and the modal angle $\theta$ satisfy the Bragg condition $\lambda_{0,\pm1} = 2n\Lambda_{0,\pm1}\sin\theta$ , where $n$ is the effective index of the waveguide. The sampling period is obtained from Eq. (5). The transmission spectrum and modal gain are calculated using the transfer matrix method (TMM) [3,16] with the incident wavelength fixed at 1550 nm.

The + $1^{st}$ order subgrating is used as TBR waveguide in our design. As shown in Fig. 2, there is a transmission peak around 15° in the + $1^{st}$ order subgrating, which is caused by the π equivalent phase shift. The corresponding modal gain is −13.43 $m^{-1}$, which indicates a dominant resonant mode along the transverse direction.

**Table 1. Parameters used in the simulation**

| | |
|---|---|
| Modal angle $\theta$ | 15° |
| Grating period $\Lambda_0$ | 985.83 nm |
| Grating period $\Lambda_{+1}$ | 937.45 nm |
| Sampling period $P$ | 19.1 μm |
| Average dielectric constant $\varepsilon_{r0}$ | 10.2028 |
| Amplitude of dielectric constant | 0.1579 |
| Laser width $W$ | 150 μm |

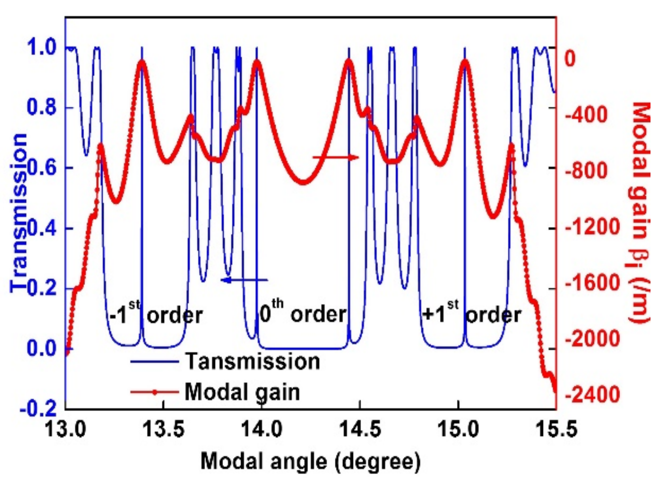


Fig. 2. Calculated transmission spectrum and modal gain of the proposed TBR waveguide.

However, as analyzed above, there are the other three potential guided modes, i.e., one in the $-1^{st}$ order subgrating and two at the edges of the $0^{th}$ order subgrating, which have similar modal gains as the + $1^{st}$ order resonant mode as listed in Table 2. Therefore, the TBR waveguide with sampled grating can be considered as a four-mode waveguide. As a result, multimode resonance may occur in this waveguide. If single mode resonance is required, the $0^{th}$ order and the $-1^{st}$ order resonant modes can be suppressed by angled facets. The detail analysis will be discussed in the following section [1,17]. It should also be noted that the TBR guided mode is different from the TIR guided mode. They are lossy due to the distributed reflection of the Bragg grating with a finite width.

**Table 2. Calculated modal gains of the ± 1st and 0th order subgratings**

| Subgrating order | $-1^{st}$ | $0^{th}$ | $0^{th}$ | $+1^{st}$ |
|---|---|---|---|---|
| Modal angle | 13.39° | 13.98° | 14.44° | 15.035° |
| Modal gain $\beta.(m^{-1})$ | −19.04 | −17.42 | −12.88 | −13.43 |

The normalized electric field of the + 1$^{st}$ order resonant mode in the transverse direction is calculated as shown in Fig. 3(a). It possesses a fast spatial oscillation due to the grating effect. Particularly, a stair-like envelope can be seen, which is caused by the sampling pattern. It shows that the power changes rapidly in the region with grating but is nearly constant in the region without grating. Figure 3(b) shows the normalized amplitude of the forward and backward electric fields.

An effective modal width is usually defined to compare the light confinement ability in TBR waveguide [10]. Since there is an equivalent π phase shift in the proposed structure, one can regard the center region with the strongest electric field amplitude in Fig. 3(a) as the waveguide core with a width of $P$. Then the sampled grating on each side of the core is considered as the waveguide cladding.

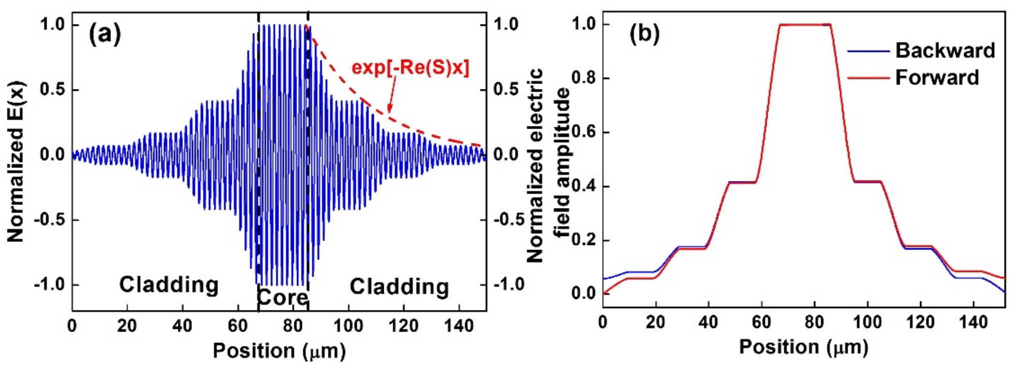


Fig. 3. (a) Normalized $E(x)$ and (b) normalized electric field amplitude of the + 1st order resonance mode.

The envelope of the electric field profile in the grating can be well approximated by an exponential decay $\exp\left[-\mathrm{Re}(S)x\right]$ as shown by the red dashed line, where $S=\left[\kappa_{+1}^{2}+(\gamma-i\Delta k)^{2}\right]^{1/2}$, $\kappa_{+1}$ is the coupling coefficient of the + 1$^{st}$ order subgrating, $\gamma$ is the transverse modal gain, $\Delta k=k_{x}-k_{b}$ is the detuning wave vector and $k_{x}$ is the $x$ component of the wave vector. Then we define the effective modal width of the proposed laser as $w_{e}=P+2/\mathrm{Re}(S)$, while the field penetration depth in the grating is $1/\mathrm{Re}(S)$. We calculated the effective modal width with different etch depth of the grating as listed in Table 3. It can be seen that the modal width decreases with the increasing of the etch depth, which means a stronger light confinement in the waveguide core. However, a large etch depth means that the grating is close to the active region, and it increases the scattering loss due to the imperfect fabrication. Therefore, the etch depth should be optimized according to the practical devices.

**Table 3. Effective modal width with different etch depth**

| Etch depth (nm) | $\Delta n$ | $\kappa_{+1}(1/cm)$ | $\gamma(/cm)$ | $w_e(\mu m)$ |
|---|---|---|---|---|
| 700 | 0.009487 | 497.4/π | 26.421 | 143.65 |
| 750 | 0.012096 | 634.6/π | 14.682 | 117.81 |
| 800 | 0.015402 | 808.8/π | 6.625 | 96.74 |
| 850 | 0.019588 | 1029.9/π | 2.204 | 80.09 |
| 900 | 0.024716 | 1301.8/π | 0.491 | 67.37 |

The product of the coupling coefficient and the TBR waveguide width $\kappa_{+1}W$ is an important factor in the design. If $\kappa_{+1}W$ is small, the transverse confinement is not strong enough to support the lasing action with a low threshold. Otherwise, high order spatial modes can occur and spatial hole burning becomes serious if $\kappa_{+1}W$ is too large. For a practical design, the condition $2 \le \kappa_{+1}W \le 10$ is usually preferred [18]. We choose an etch depth of 900 nm in our design and the corresponding $\kappa_{+1}W$ is around 6.22. It should be noted that the coupling coefficient of the sampled grating is lower than that of the uniform grating, so the transverse size of the proposed laser is wider than the TBR laser with uniform grating.

## 4. Discussions

### *4.1 Small modal angle (SMA) mode*

Besides the TBR modes analyzed above, there exist some other modes with very low radiation loss, which propagate along the cavity with small modal angles and may resonant together with the desired TBR mode [1]. We calculated the modal gains of all the TBR and SMA modes in Fig. 4. In addition, the modal gains of the TBR waveguide with sampled and uniform grating are both calculated. There are some peaks in the modal gain curve of the sampled grating due to the high order Fourier components, which agrees well with the above analysis. While the modal gain curve of the uniform grating has only one dominant peak around the Bragg wavelength.

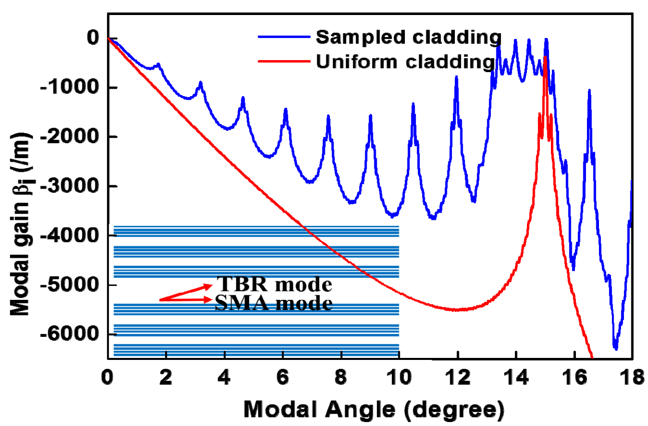


Fig. 4. Modal gain versus modal angle for the TBR waveguide with sampled grating and uniform grating. The inset shows the difference between TBR mode and SMA mode.

### *4.2 Facet reflection*

There are mainly three methods or a combination of them to provide longitudinal feedback for the TBR lasers, i.e., angled facet, facet coating and longitudinal grating. Among them, the mode selectivity of facet coating is relatively low, and the fabrication of longitudinal grating is complicated. Therefore, we use an angled facet as a spatial filter to select the longitudinal mode in the design.

The reflection coefficient of different modes at an angled facet can be calculated by $R = R_f(\theta)\cdot r_f$, where $R_f(\theta)$ is the Fresnel reflection coefficient and $r_f$ is given by [5]:

$$r_f = \frac{\mathrm{Re}(\beta)}{2\omega\mu_0 P_0}\int_{-\infty}^{+\infty} E_f(x)E_b(x)e^{i2\mathrm{Re}(\beta)\sin(\alpha-\theta)x}dx \tag{13}$$

where $\mathrm{Re}(\beta)$ is the real part of the propagation constant, $\omega$ is the angular frequency, $\mu_0$ is the magnetic permeability of vacuum, $P_0$ is the power carried by the guided mode, $E_f(x)$ and $E_b(x)$ are the forward and backward electric field respectively, $\alpha$ is the facet angle as shown in the inset of Fig. 5, and $\theta$ is the modal angle.

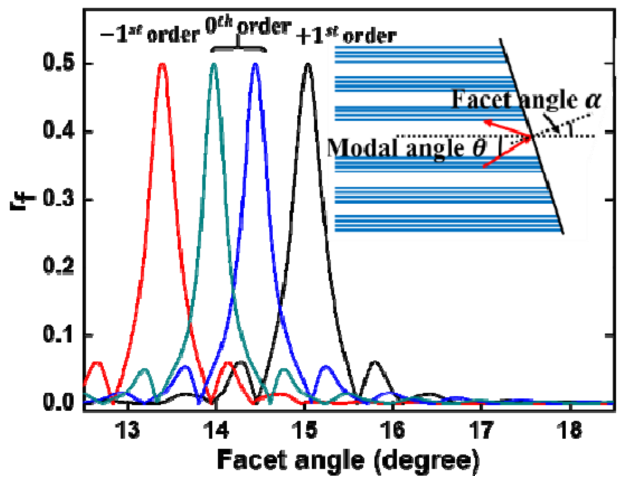


Fig. 5. The $r_f$ of the facet with different facet angles. The inset shows the top view of the grating with angled facet.

We calculated $r_f$ versus the facet angle for the ± $1^{st}$ order and the $0^{th}$ order resonant modes as shown in Fig. 5. It can be seen that $r_f$ possesses a maximum value around 0.5 when the facet angle equals to the modal angle of each mode, which proves that the angled facet is an effective method to select the desired mode. The + $1^{st}$ order resonant mode is selected when the facet angle is around 15°, while the $-1^{st}$ order and the $0^{th}$ order resonant modes are fully suppressed. It should be mentioned that the reflection of the angled facet is different from that of the standard DFB laser. There is some additional loss due to the misalignment of the phase fronts [17]. Since the incident light in consideration is nearly normal to the facet, the dependence of $R_f(\theta)$ on incident angle can be neglected [5]. When the effective index is 3.2, $R_f(\theta)$ is around 0.5238 and the reflectivity from one facet is around 0.0686. However, it can be increased by high-reflection coating at the facets.

It is also shown in Fig. 5 that there are some overlap between the $r_f$ curves of each mode, which can cause mode coupling when the facet angle is not well controlled during fabrication. For instance, both the + $1^{st}$ order and the $0^{th}$ order mode can resonant when the facet angle is around 14.8°, which results in a snake-like appearance of the whole mode profile. The variation period of the field distribution for beating two modes is defined as the beat length [3],

$$L_{beat} = \frac{2\pi}{|\beta_{m+1}-\beta_m|} \tag{14}$$

Optics EXPRESS

where $\beta_{m+1}$ and $\beta_m$ are the propagation constants of the two modes. The beat length is approximately 184 μm for the + 1$^{st}$ order mode and the blue side of the 0$^{th}$ order mode in our design. When the laser length is designed to be multiple times of the beat length, the modal angle of the beating mode is an average value of the modal angles of the two separated modes.

The overlap of $r_f$ curves can be controlled by changing the 0$^{th}$ order grating period, which determines the sampling period and the modal angle deference between the + 1st order mode and the 0th order mode according to Eq. (5). For example, if the 0$^{th}$ order grating period is designed to be 1046.3 nm instead of 985.83 nm, the sampling period is 9 μm and the modal angle difference is around 1.3°, and then the $r_f$ curves of each mode are fully separated. In addition, we suggest that the 0$^{th}$ grating period should be less than 1764.2 nm in order to keep the sampling period above 2 μm, which can be easily realized by conventional photolithography.

However, small modal angle difference also shows an advantage that the fabrication tolerance of the facet angle can be relaxed. The laser operates provide that the facet angle is between 13.4° and 15° (the corresponding modal angles of the ± 1$^{st}$ order modes) in our design instead of a narrow facet angle range for conventional TBR waveguide lasers.

It should be also mentioned that $r_f$ is nearly zero for the SMA modes, which means the SMA modes can be well suppressed by the angled facet.

### *4.3 Spatial hole burning*

Spatial hole burning (SHB) effect usually exists in DFB lasers and may deteriorate the laser performance, such as the single longitudinal mode (SLM) stability. The nonuniform light intensity leads to a nonuniform refractive index distribution due to the Kramer-Kroenig relationship [15]. A practical method to reduce the SHB is decreasing the coupling coefficient around the core region, which can be realized by changing the duty cycle of the sampling pattern. Since there are only a few sampling periods in the designed structure, we only change the duty cycles of the two sampling periods around the core region symmetrically as shown in the inset of Fig. 6, keeping the duty cycle of the grating region as 0.5. A normalized flatness value $F$ is defined to compare the SHB effect of different duty cycles [19],

$$F = \frac{1}{W}\int_0^W \left[P(x) - \overline{P}\right]^2 dx \tag{15}$$

where $W$ is the cavity width, $P(x)$ is the power distribution and $\overline{P}$ is the average of $P(x)$.

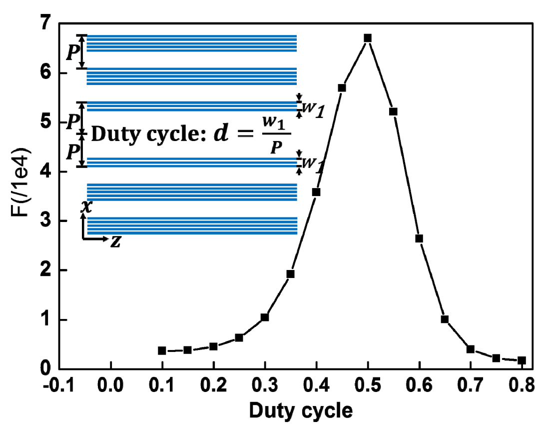


Fig. 6. The normalized flatness value with different duty cycles. The inset shows the structure of the grating.

Optics EXPRESS

It can be seen in Fig. 6 that the maximum flatness value occurs when the duty cycle is 0.5, which means a strong SHB effect. Besides, the flatness value decreases one order of magnitude when the duty cycle is below 0.26 or above 0.67. Therefore, the SHB effect can be effectively reduced by designing the duty cycle of the sampling pattern. In addition, the simulation shows that the flatness value of an actual phase shift grating is higher than the maximum value of the sampled grating.

### *4.4 Near field and far field beam patterns*

The near field and far field beam patterns of the TBR laser with sampled grating are a little different from that of the TBR laser with uniform grating. The near field pattern is calculated based on the Huygens-Fresnel principle and shown in Fig. 7(a). There are small ripples due to the stair-like electric field profile in the sampled grating, which agrees well with Fig. 3. However, the ripples nearly vanish when the light propagates far away from the facet. As is plotted in Fig. 7(b) when z = 5000 μm, a far field beam pattern with very small side lobes is achieved.

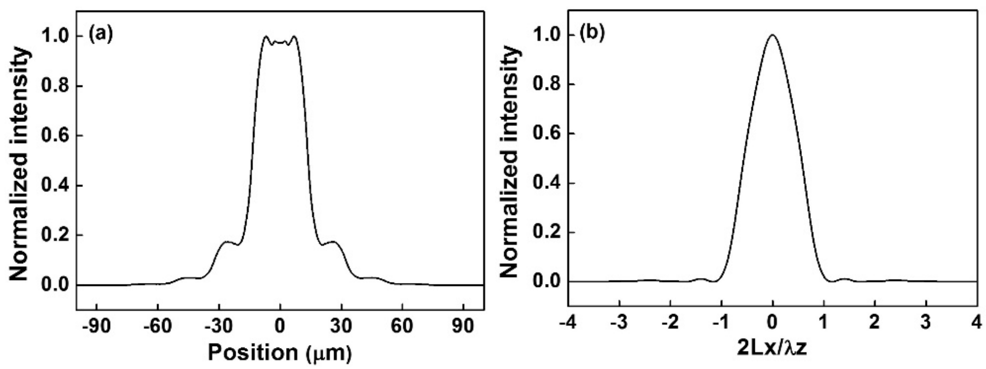


Fig. 7. Calculated (a) near field and (b) far field beam patterns of the proposed TBR laser.

## 5. Conclusion

A TBR waveguide semiconductor laser with sampled grating is proposed and analyzed. The π phase shift is equivalently realized by shifting half of the sampling period, while the basic grating is uniform. Combining the spatial filter such as the angled facet, single transverse mode resonance can be realized. Thanks to the sampled grating structure, the fabrication processes can be greatly simplified to one step holographic exposure and another step of micrometer-scale lithography. Therefore, the proposed structure would be helpful for wide-stripe high power semiconductor lasers. It should be mentioned that although the analysis above is for TE polarization, the sampled grating can also be used in TM polarized devices such as tensile strained semiconductor lasers and quantum cascade lasers with a modification of the effective index.

## Funding

Chinese National Key Basic Research Special Fund (2017YFA0206401); Natural Science Foundation of Jiangsu Province of China (BK20160907); National Natural Science Foundation of China (NSFC) (61435014, 61504058, 61504170); NUPTSF (NY216013, NY217049).